Available online at www.sciencedirect.com
ScienceDirect
Thermochimica Acta 455 (2007) 60–65
thermochimica acta
www.elsevier.com/locate/tca

The measurements of thermal diffusivity dependent on temperature for pure metals by the new photothermal displacement configuration

K.J. Lee [a], J.W. Kang [b], P.S. Jeon [b], H.J. Kim [c,*], J. Yoo [c]

[a] *R & D Center LG Micron Ltd., 407, Anyang-Megavalley Bldg., Anyang 431-804, Republic of Korea*
[b] *Department of Mechanical Engineering, Ajou University, Wonchun-dong, Yeongtong-gu, Suwon 443-749, Republic of Korea*
[c] *Division of Mechanical Engineering, Ajou University, Wonchun-dong, Yeongtong-gu, Suwon 443-749, Republic of Korea*

Available online 8 January 2007

Abstract

The photothermal displacement method has been known as a useful technique to measure the thermal properties, such as thermal conductivity and thermal diffusivity. However, the previous measurements of thermal properties have been performed only at a room temperature. But these would be not valid for all the temperature range because the different heat transfer mechanism by the phonon and phonon–electron scattering occurs at a high temperature in a microscopic view. In order to obtain the thermal diffusivity of pure metals in correspondence to the temperature increase, the surroundings of the sample should be heated and kept at steady state temperature conditions. Therefore, in this study, the new experimental equipment is designed to satisfy such conditions. And the thermal diffusivities for four kinds of pure metals in the temperature range 300–673 K are measured with high accuracy using the photothermal displacement method.

Keywords: Photothermal displacement; Thermal diffusivity; Probe beam deflection; Thermoelastic deformation; Phase difference

1. Introduction

The measurement technique of thermal properties using photothermal effects has been suggested with various methods until now. During 1980–1990, analysis of theoretical model based on the principle of measurement has been performed and identified the possibility of measurements with the simple experiment [1–5].

In the latter half of 1990, the thermal diffusivity became to be measured quantitatively with the delicate experimental device and the raw data processing [6,7]. After 2000, the measurement was focused to expand the application range for various types of materials.

Looking into the measurable materials, it became possible to measure the thermal properties of liquid or gas materials [8,9] and the solid materials and such as metals, nonmetals, semiconductors and bi-layer materials with thin film [10–12].

Also, the measurement of thermal properties was applied to investigate the characteristics of heat transfer for the materials which have a microstructure or nanostructure [13–15].

However, previous results of thermal properties have been measured in a room temperature. Although the thermal diffusivity of the material was previously known, it will have a wholly different thermal diffusivity in a high temperature.

Therefore, in this study, the photothermal displacement system with the high accuracy, which can measure the thermal diffusivity for the heated sample, is developed. Using the developed system, the thermal diffusivity of pure metals, in accordance with the temperature change, is measured.

2. Theory and principle

The principle for photothermal displacement method is schematically illustrated in Fig. 1. When the modulated pump beam is incident on the sample surface, the energy is absorbed by the sample, which then gives a rise to the temperature increase. This temperature change of the sample induces the thermoelastic deformation on the surface of the sample and such thermoelastic deformation depends on the thermal and optical properties of the

* Corresponding author. Tel.: +82 31 219 2340; fax: +82 31 213 7108.
E-mail address: hyunkim@ajou.ac.kr (H.J. Kim).

0040-6031/$ – see front matter © 2007 Elsevier B.V. All rights reserved.
doi:10.1016/j.tca.2006.12.019

Nomenclature

a	radius of the pump beam (m)
f	modulation frequency (Hz)
J_o	zero-order Bessel function
J_1	first-order Bessel function
k	thermal conductivity (W/m K)
L	thickness of sample (m)
L_{th}	thermal diffusion length (m)
$P(t)$	wave shape of heat source (W)
P_0	power of the pump beam (W)
Q	heat source (W/m^3)
R	reflectivity
t	time (s)
T	temperature (K)
u	displacement (m)

Greek symbols

α	thermal diffusivity (m^2/s)
α_{th}	thermal expansion coefficient (K^{-1})
δ	integration variable
ζ	deformation gradient (radian)
η_p	eigenvalue of z direction
θ	phase difference (°)
λ	optical absorption coefficient (m^{-1})
ν	Poisson's ratio
σ	stress (N/m^2)
ω	angular frequency (s^{-1})

sample such as thermal diffusivity and the absorption coefficient and so on. And neglecting the refraction by air on the surface of sample, the difference of angle (ζ) between the incidence and reflection beam is proportional to the gradient of deformation ($= \mathrm{d}u/\mathrm{d}r$) as shown in Eq. (1).

$$\zeta = 2\frac{\mathrm{d}u}{\mathrm{d}r}\bigg|_{z=0} \tag{1}$$

Using the relation such as shown in Eq. (1), the thermal diffusivity can be determined by the comparison of the experimental and theoretical values. In order to obtain the thermal diffusivity in theory, the analysis of the temperature distribution onto the sample should be carried out first. And then, apply the temperature distribution result to the thermoelastic equation to obtain the formula for deformation gradient.

To obtain the temperature distribution and the deformation gradient of the sample, a two-dimensional cylindrical solid model, which has a homogeneous and isotropic infinite plate with the finite thickness L and stress-free boundaries were chosen as shown in Fig. 1.

The governing equation is the 2D cylindrical heat conduction equation with a heat source as shown in Eq. (2). The heat source is expressed as shown in Eq. (4) using the radius of pump beam with a Gaussian profile and the exponential function of optical absorption coefficient. The adiabatic condition is applied as the boundary condition as shown in Eq. (3). When the analysis of temperature distribution was conducted, the effects of the convection and radiation heat transfer were neglected [16,17].

$$\nabla^2 T(r,z,t) + \frac{1}{k}Q(r,z,t) = \frac{1}{\alpha}\frac{\partial T(r,z,t)}{\partial t} \tag{2}$$

$$k\frac{\partial T}{\partial z}\bigg|_{z=0,L} = 0 \tag{3}$$

$$Q(r,z,t) = \frac{\lambda P_0(1-R)}{4\pi a^2}\,\mathrm{e}^{(-r^2/a^2)-\lambda z}(1+\cos(\omega t)) \tag{4}$$

Applying the result for the temperature to the thermoelastic equation as shown in Eq. (5) and then solving the equation of thermoelastic deformation with a free stress boundary condition as shown in Eq. (6), the final equation, Eq. (7) about deformation gradient is obtained [16,18].

$$(1-2\nu)\nabla^2\vec{u} + \nabla(\nabla\vec{u}) = 2(1+\nu)\alpha_{th}\nabla T \tag{5}$$

$$\sigma_{rz}|_{z=0,L} = 0, \qquad \sigma_{zz}|_{z=0,L} = 0, \tag{6}$$

$$\frac{\partial u_z}{\partial r}\bigg|_{z=0} = \frac{(1+\nu)\alpha_{th}P\lambda^2}{2\pi kL}\int_0^\infty \frac{\delta^2 J_1(\delta r)\,\mathrm{e}^{-\delta^2 a^2/4}}{\lambda^2-\xi^2} \times \sum_{p=1}^{\infty}\frac{\eta_p^2 H(\delta)[(-1)^p - \cosh(\xi L)]}{\xi(\delta^2+\eta_p^2)(\xi^2+\eta_p^2)\sinh(\xi L)}\,\mathrm{d}\delta \tag{7}$$

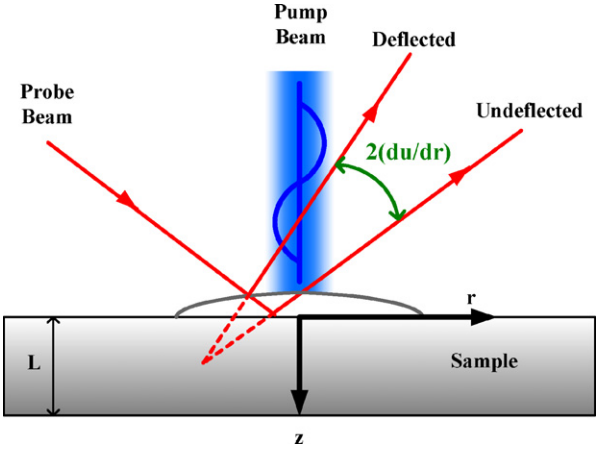

Fig. 1. The principle of a measurement and theoretical model.

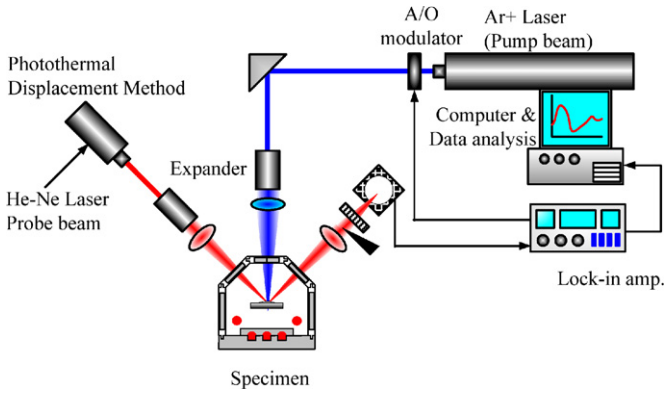

Fig. 2. Photograph of experimental setup installed in the heating chamber.

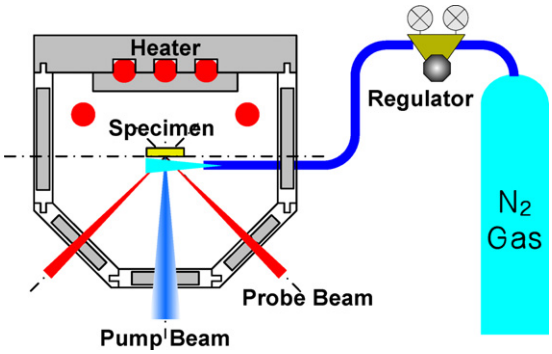

Fig. 3. Injection of N_2 gas into the heating chamber.

where

$$H(\delta) = \frac{\sinh^2(\delta L) + (-1)^p \delta L \sinh(\delta L)}{\delta^2 L^2 - \sinh^2(\delta L)}, \quad \eta_p = \frac{p\pi}{L} \tag{8}$$

Then, the phase difference can be formulated by the ratio of imaginary to real part of the probe beam deflection angle as the following. Note that Eq. (9) is the function of a thermal diffusivity, α.

$$\theta(r, f, a, \alpha, t) = \tan^{-1}\left[\frac{\mathrm{Im}\{(\mathrm{d}u/\mathrm{d}r)_{z=0}\}}{\mathrm{Re}\{(\mathrm{d}u/\mathrm{d}r)_{z=0}\}}\right] \tag{9}$$

3. Experimental apparatus

Fig. 2 shows the experimental apparatus in which the heating chamber is optically aligned and installed. The pump beam, as a heating source, is a continuous Ar-ion laser with 488 nm wavelength and 1.3 mm diameter with Gaussian distribution. The pump beam is modulated as a sine wave using A/O modulator, controlled by lock-in amplifier. This modulated beam is focused on the sample surface with 120–140 μm diameter and the beam power reaches the sample surface with 0.3 W after passing through the acousto-optic (A-O) modulator, mirrors, expander and lens. It is critically important for the pump beam to be adjusted perpendicular to the sample surface.

The probe beam is provided by a He–Ne laser with 633 nm wavelength and 5 mW power. The probe beam line is aligned to the sample surface with 45° angle. And the probe beam is focused with 30 μm through the combination of lens.

In order to change the relative distance between the pump and probe beam, the probe beam is fixed. And the pump beam including the mirror, expander and lens and the sample are set together on the autolinear translation stage to move in r direction with 0.2 μm resolution simultaneously. The driver of autolinear stage is connected to the personal computer for feed back control. Therefore, the exact relative position between pump and probe beam can be controlled and ensured in real time.

Table 1
Thermal diffusivity of pure metals

Pure metals	α_{liter} ($\times 10^{-5}$ m^2/s)	α_{meas} ($\times 10^{-5}$ m^2/s)	R.E. (%)
Ag	17.3	17.579	1.6
Cu	11.6	11.544	0.5
Fe	2.3	2.332	1.4
Ni	2.3	2.327	1.2
Zn	4.4	4.429	0.6

R.E.: relative error [19,20].

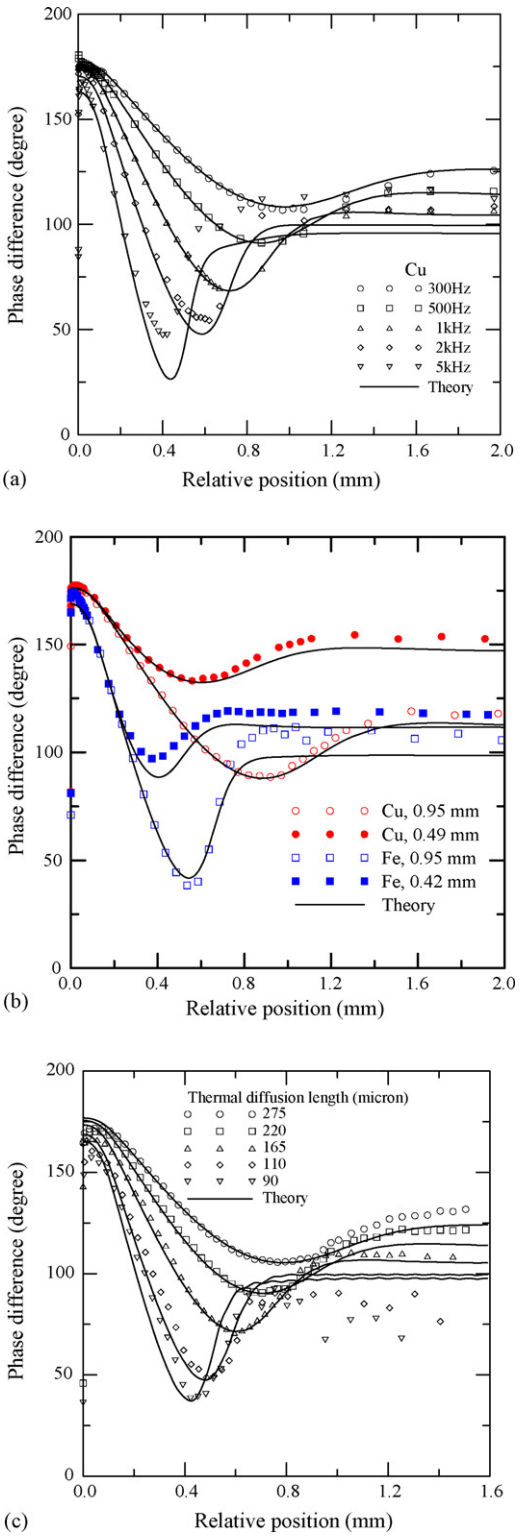

Fig. 4. Influence of each parameter f, L and L_{th} on the phase difference curve. (a) Effect of frequency f. (b) Effect of sample thickness L. (c) Effect of thermal diffusion length L_{th}.

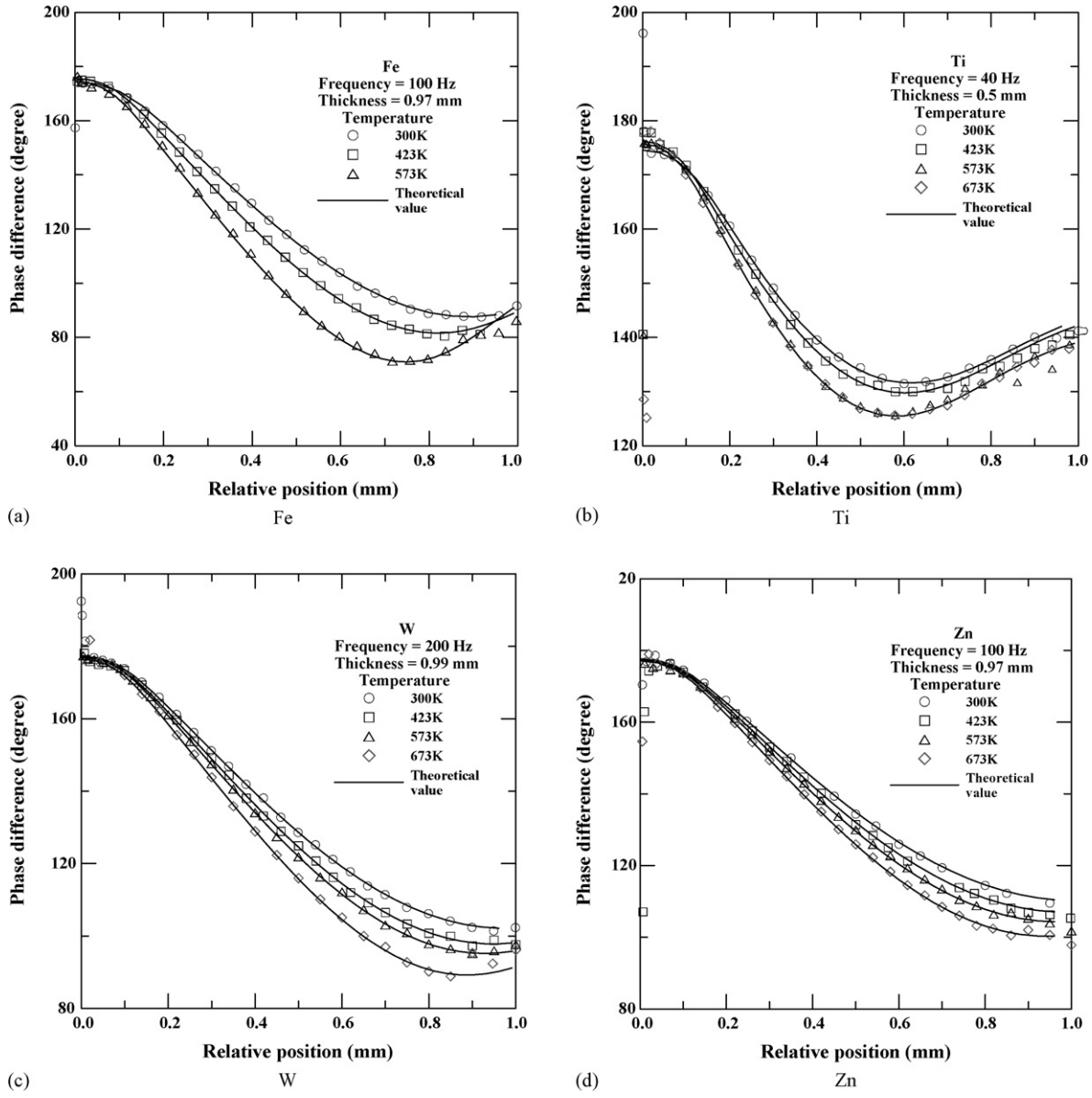

Fig. 5. Phase differences for pure metals as the function of a temperature.

The signal emerging from the detector is coupled with the amplifier and is measured by the lock-in amplifier.

To increase the temperature of the sample from 300 to 673 K, the heating chamber is devised as shown in Fig. 3. Five cartridge heaters with 1 kW power are adhered to the inner side of heating chamber. Consequently, the sample in the chamber is heated by the radiation and convection heat transfer. The chamber is designed to consider the optical alignment and the injection line of N_2 gas as shown in Figs. 2 and 3. In order to minimize the oxidation of the sample by the air in the chamber the N_2 gas is injected to near the front surface of the sample at very low speed.

As the samples, Ag, Cu, Fe, Ni, Ti, W and Zn with above 99.98% purity are used and polished with alumina powder to avoid the local change of optical properties on the surface. Above pure metals are adopted to the measurement of thermal diffusivity at room temperature and then each values are compared with the literature values. Also, thermal diffusivities of Fe, Ti, W and Zn are measured at room temperature (300 K), 423, 573 and 673 K to obtain thermal properties in accordance with temperature changes.

4. Results and discussion

4.1. Parametric study

To optimize the experimental measurement condition, the parametric study was conducted. The phase difference is a function of various parameters as shown in Eq. (9). The influence of each parameter on the phase difference was examined through the experiment, neglecting the effect of pump beam diameter a. As a result, it was found that the modulation frequency f and the sample thickness L have a large effect on the phase difference as shown in Fig. 4a and b. Also, the result for the influence

Table 2
Thermal diffusivity of pure metals as the function of a temperature

Pure metals	Thermal diffusivity ($\times 10^{-5}$ m^2/s)											
	300 K			423 K			573 K			673 K		
	L	*M*	R.E.	*L*	*M*	R.E.	*L*	*M*	R.E.	*L*	*M*	R.E.
Fe	2.30	2.29	0.4	1.71	1.82	6.4	1.28	1.31	2.3	1.21		
Ti	0.97	0.96	1.0	0.81	0.87	0.87	0.74	0.74	0.1	0.71	0.74	4.2
W	6.97	6.90	1.0	6.05	6.14	6.14	5.26	5.68	8.0	4.90	4.76	2.9
Zn	4.37	4.40	0.7	3.96	3.89	3.89	3.47	3.53	1.7		3.14	

M, measured value; *L*, literature; R.E., relative error [19,20].

of thermal diffusion length is shown in Fig. 4c. When the thermal diffusion length is longer or the frequency is lower, the experimental phase difference values agree much better with the theoretical value. Because the thermal diffusion length is the function of frequency and thermal diffusivity ($L_{\text{th}} = \sqrt{\alpha/\pi f}$), the higher the modulation frequency is, the shorter the thermal diffusion length becomes. Also, the measurable relative position by the thermoelastic deformation is shorter. Therefore, the frequency of the modulated beam is set to less than 200 Hz for the measurement in Section 4.2.

The quantitative thermal diffusivities of pure metals are measured and listed in Table 1 through the developed photothermal displacement method. The comparison of the literature thermal diffusivity (α_{liter}) with the measured thermal diffusivity (α_{meas}) shows within 1.6% of relative errors (R.E.).

4.2. Thermal diffusivity as the function of a temperature

Fig. 5 shows the results of phase differences along with the relative position between pump and probe beam at each temperature. Fe, Ti, W and Zn were used for samples and measurements were done at 300 K, 423, 573 and 673 K. To ensure the set temperature, the experiment was carried out after the inside of the chamber as well as the samples, reached the steady state of each set temperature.

At the same relative position, as the temperature of the sample increased, the phase difference enlarged. The increase of phase difference means that the thermal diffusivity decreases because the thermoelastic deformation occurs slowly according to the decrease of thermal diffusivity.

The quantitative thermal diffusivity was determined by using the curve fitting obtained from the measured and theoretical values of phase difference. The measured thermal diffusivity is shown in Fig. 6 and Table 2 per each temperature.

Fig. 6 shows that the measured thermal diffusivities were compared with the fitting curve of literature value versus the temperature. The fitting curve was obtained from the thermal diffusivity which is calculated from the thermal conductivity, the specific heat and the density at each temperature in the literature [19,20].

According to the temperature increase, it shows that the decreasing rate of thermal diffusivity for the metals is different at each sample. In other words, the thermal diffusivity changes not linearly versus the temperature. The rate of thermal diffusivity decreasing is analogous to the values in the literature. In

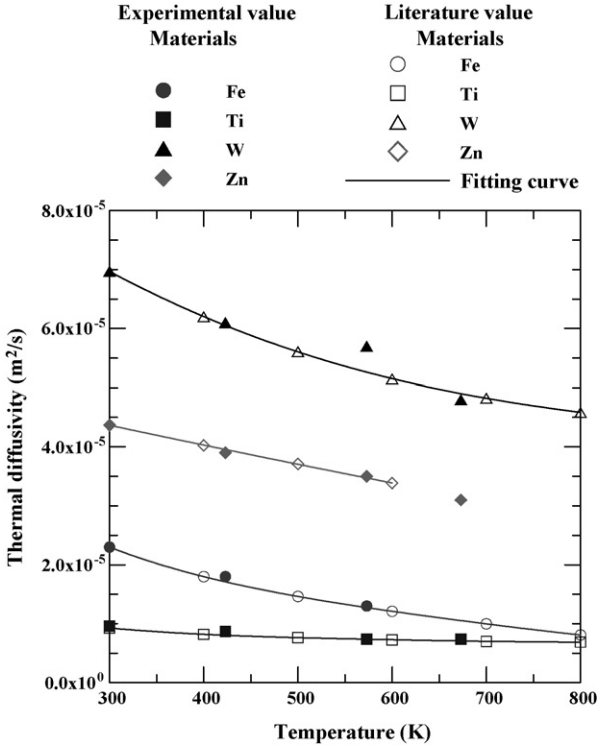

Fig. 6. Comparison of measured and literature thermal diffusivity as the function of a temperature.

Table 2, those quantitative values are compared with literature data. The average of relative errors between them is calculated at 3.5%.

5. Conclusion

In conclusion, we improved the method for the determination of thermal diffusivity using the photothermal displacement method. To obtain the thermal diffusivity from the measured phase difference by photothermal displacement method, the theoretical analysis has been achieved with a parametric study. The curves between the theoretical and measured phase differences are matched very well and the quantitative thermal diffusivity can be determined for pure metals. Additionally, we developed the method for the determination of thermal diffusivity as the function of a temperature using the photothermal displacement technique. When the temperature of sample increases, the thermal diffusivity decreases, showing that the decreasing rate of

thermal diffusivity for the metals versus a temperature is not linear.

Therefore, it is considered that the thermal diffusivity of pure metals and new materials in a high temperature must be measured. Therefore, this technique can give one of solutions to measure the thermal diffusivities of pure metals and new materials and to understand the heat transfer mechanism in a high temperature.

Acknowledgements

This work was supported by Grant No. R01-2006-000-11264-0(2006) from the Basic Research Program of the Korea Science & Engineering Foundation and the Grant of Korea Science Engineering Foundation (R05-2004-000-11406).

References

[1] J. Opsal, A. Rosencwaig, J. Appl. Phys. 53 (1982) 4240.
[2] J. Opsal, A. Rosencwaig, D.L. Willenborg, Appl. Opt. 22 (1983) 3169.
[3] M.A. Olmstead, N.M. Amer, S. Kohn, J. Appl. Phys. (A) 32 (1983) 141.
[4] D.L. Balageas, J.C. Krapez, P. Cielo, J. Appl. Phys. 59 (1986) 348.
[5] B. Li, Z. Zhen, S. He, J. Phys. 24 (1991) 2196.
[6] G.L. Bennis, R. Vyas, R. Gupta, S. Ang, W.D. Brown, J. Appl. Phys. 84 (1998) 3602.
[7] E.T. Ogawa, C. Hu, P.S. Ho, J. Appl. Phys. 86 (1999) 6018.
[8] B.C. Li, R. Gupta, J. Appl. Phys. 89 (2001) 859.
[9] J. Soldner, K. Stephan, Int. J. Therm. Sci. 43 (2004) 1037.
[10] A. Mathew, J. Ravi, K.N. Madhusoodanan, K.P.R. Nair, T.M.A. Rasheed, Appl. Surf. Sci. 227 (2004) 410.
[11] V. Anjos, M.J.V. Bell, E.A. de Vasconcelos, E.F. da Silva Jr., A.A. Andrede, R.W.A. Franco, M.P.P. Castro, I.A. Esquef, R.T. Faria Jr., Microelectron. J. 36 (2005) 977.
[12] J. Martan, N. Semmar, C. Leborgne, E. Le Menn, J. Mathias, Appl. Surf. Sci. 247 (2005) 57.
[13] J.L. Nzodoum Fotsing, B.K. Bein, J. Pelzl, Superlattice Microstruct. 35 (2004) 419.
[14] D. Rochais, H. Le Houëdec, F. Enguehard, J. Jumel, F. Lepoutre, J. Phys. D: Appl. Phys. 38 (2005) 1498.
[15] X. Chen, J. Zhu, G. Yin, L. Zhao, Mater. Lett. 60 (2006) 63.
[16] P. Jeon, K. Lee, J. Yoo, Y. Park, J. Lee, Trans. KSME 26 (2) (2002) 302.
[17] Y. Bayazitoglu, M. Ozisik, Elements of Heat Transfer, McGraw-Hill, New York, 1998.
[18] W. Nowacki, Thermoelasticity, second ed., Pergamon Press, 1986.
[19] J.F. Shackelford, CRC Material Science and Engineering Handbook, CRC Press, 1994.
[20] American Institute of Physics, American Institute of Physics Handbook, Colonial Press, 1972.